John Carroll University

Carroll Collected

Faculty Bibliographies Community Homepage

2020

Measurements of branching fractions, absolute transition probabilities and J-file sum rule for the 4p(5)5p -> 4p(5)5s transitions array in neutral krypton

Haroon Asghar

Naveed K. Piracha

Raheel Ali

M. Aslam Baig

Measurements of branching fractions, absolute transition probabilities and *J*-file sum rule for the $4p^5 5p \rightarrow 4p^5 5s$ transitions array in neutral krypton

Haroon Asghar[1,2], Naveed K. Piracha[3], Raheel Ali[1] and M Aslam Baig[2]

[1] Atomic and Molecular Physics Laboratory, Quaid-i-Azam University, Islamabad 45320, Pakistan

[2] National Center for Physics, Quaid-i-Azam University Campus, Islamabad 45320, Pakistan

[3] Department of Physics, John Carroll University, University Heights, Ohio, OH 44118, United States of America

E-mail: baig@qau.edu.pk and baig77@gmail.com

Abstract

We present new results of transition rates for twenty two electric dipole transitions of neutral krypton associated with the $4p^5 5p$–$4p^5 5$ s configurations-based levels covering the wavelength region from 500 to 1000 nm using a krypton filled hollow cathode discharge lamp coupled with a set of four miniature spectrometers. The branching fractions of various dipole allowed transitions were extracted using the observed line intensity ratios, whereas, the absolute values of the transition probabilities were deduced from the measured branching fractions in combination with the known lifetimes of the upper levels. The experimental data are in good agreement with that calculated in the intermediate angular momentum coupling scheme. In addition, line strengths for all the transitions have been extracted using the measured transition probabilities. The *J-file* sum rule was also tested for each level attached to the $4p^5 5p$–$4p^5 5$ s configurations based on the recently measured and calculated normalized multiplet strengths.

Keywords: krypton, hollow cathode discharge, branching fractions, transition probabilities, relative line strengths, *J*-file sum rule

(Some figures may appear in colour only in the online journal)

1. Introduction

Transition probabilities, branching fractions (BF), oscillator strengths and relative line strengths of spectral lines are the parameters which relate to the probabilities of transitions in a given spectrum. A precise knowledge of these parameter is of paramount importance in astrophysics, plasma physics and atomic physics [1–3]. Numerous efforts have been made, both experimentally as well as theoretically to extract these parameters using the optical emission spectroscopy. Krypton is particularly important because there are several strong emission lines that lie in the infrared region due to de-excitation from the $4p^5 5p$ upper configurations-based levels to the $4p^5 5$ s lower configuration-based levels. Experimentally, the upper levels get populated by running a mild discharge in krypton and subsequently the electrons decay to the lower levels mostly through the electric dipole transitions.

Extensive work has been done in the past by many researchers to measure accurate transition rates of neutral krypton. The Roschdestwensky anomalous dispersion 'hook method' [4] was used to obtain the relative atomic oscillator strength values for a group of lines arising from transitions between the two lowest excited configurations, $np^5(n + 1)s$ and $np^5(n + 1)p$, in neon, argon and krypton. Transition probabilities and oscillator strengths of several infrared transition arrays in

Ne I and Ar I and for the visible 5p→5 s array in Kr I, were calculated using intermediate coupling approximation [5]. Transition probabilities and lifetimes of all the rare gas spectra were calculated theoretically [6]. The relative transition probabilities of 22 lines of Kr I and 33 lines of Kr II were reported by using a gas-driven shock tube as a radiation source [7]. Later, transition probabilities were computed for the Ne I, Ar I and Kr I transitions in the intermediate coupling theory including an effective operator [8]. The transition probabilities for 23 Kr I lines between 431.9 nm and 892.9 nm attached to the 5p→5 s and 6p→5 s transition arrays from the wall-stabilized arc measurements have been computed [9]. Subsequently, the transition probabilities and lifetimes for Kr I and Xe I spectra have been calculated using the Central Field Model that takes into account the intermediate coupling theory and configuration mixing scheme [10]. Absolute transition probabilities of thirteen electric dipole transitions attached with 5p→5 s transition array and lifetimes of the sixteen levels of Kr I belonging the $4p^5 5p$ and $4p^5 6p$ configuration were measured [11, 12]. Furthermore, radiative lifetimes of eight krypton levels and transition probabilities for 5p→5 s transition array of Kr I were measured by using the time resolved laser induced fluorescence technique in a flowing afterglow apparatus [13]. The relative transition probabilities for the 28 infrared lines arising from the $4p^5 6$ s and $4p^5 4d$ configuration of Kr I were measured by the emission line intensity measurements of an optically-thin light source [14]. The lifetimes of three states of Kr I were measured and the experiment was involved a pure krypton discharge at pressure ⩽15 mTorr [15]. The atomic lifetimes and individual oscillator strengths were measured for 5p configuration of Kr I by using the Beam-gas-dye laser spectroscopy as a precise, cascade-free and collision free method [16]. Furthermore, he BF and transition rates for the 5p→5 s transition array of neutral krypton were reported using a wall-stabilized electric arc and a 2-m monochromator for the spectral lines in the visible, and with a hollow cathode lamp and the NIST 2-m Fourier transform spectrometer for the lines in the near infrared region [17]. It is pertinent to mention here that the values of transition probabilities measured in [17] are listed in NIST Database [18]. Later, transition probabilities of 35 lines of krypton in the spectral region 450–580 nm were measured using the emission technique [19]. Transition probabilities of thirteen spectral line of Kr I belongs to 5p→5 s transition array of neutral krypton have been deduced using the discharge tube and stark width was also investigated [20].

In this contribution, we report new experimental results on the transition probabilities of twenty two dipole allowed transitions attached to the $4p^5 5p \rightarrow 4p^5 5$ s transition array of krypton. The absolute transition probabilities have been deduced by combining the measured BF with the lifetimes of the upper levels. The measured transitions probabilities have been transformed into relative line strengths that have been compared with the theoretical work [10] as well as with the NIST Database [18]. In addition, a comparison of the experimentally measured relative line strengths for each multiplet have been made with the normalized theoretical line strengths.

2. Experimental setup

The experimental setup used in this work consists of a commercial hollow cathode lamp (Photron, Australia) and a set of four miniature spectrometers (Ava-Spec 3648, Avantes, Netherlands). The diameter of the cathode lamp was about 3 mm that was filled with krypton at a pressure of around 5–8 torr. The lamp was operated through a regulated DC power supply, capable of delivering 200 V and 20 mA. The emission spectra were registered using a set of four spectrometers (Avantes, Netherlands) each equipped with 10 μm wide slit and covering the spectral region from 250 nm to 900 nm. The resolution of the setup is about 0.06 nm at 500 nm, measured by a narrow band width dye laser. The spectrometers were intensity calibrated by the manufacturer. The spectra were taken at varying currents for further analysis. Some spectra were also recorded using the HR4000 (Ocean Optics, USA) spectrometer covering the range from 200 to 1100 nm.

3. Results and discussions

3.1. Description of the emission spectrum of krypton

The ground state configuration of krypton is $4s^2 4p^6$ and its ground-state is $^1S_0$. The excited states are represented in the j_cK- coupling scheme; $[(\ell_1 s_1) j_c, \ell_2$ K,s_2]J in which the j_c is the angular momentum quantum number of the core electrons which is coupled with the orbital angular momentum of the excited electron ℓ_2 to form the K quantum number. Finally, K is coupled with the spin quantum number of the excited electron s_2 to yield the total angular momentum quantum number J of the level; the level are designated as $[K]_J$. The first group of excited levels are based on the $4p^5 5$ s configuration; $4p^5 5$ s$[3/2]_{2,1}$ attached to 5p ($^2P_{3/2}$) and $4p^5 5$ s'$[1/2]_{0,1}$ attached to the 5p ($^2P_{1/2}$) parent ion levels. The second group of the excited levels are based on the $4p^5 5p$ configuration; 5p$[3/2]_{2,1}$, 5p$[1/2]_{1,0}$, 5p$[5/2]_{3,2}$, built on the 5p ($^2P_{3/2}$) parent ion level and 5p'$[3/2]_{2,1}$, 5p'$[1/2]_{1,0}$ attached to the 5p ($^2P_{1/2}$) level. In Paschen notation, the $4p^5 5$ s configuration-based group is expressed as $2s_i$ ($i = 1, 2, 3, 4$) and the $4p^5 5p$ group as $2p_j$ ($j = 1, 2, 3...., 10$). It is worth mentioning here that some of the allowed lines lie above 1000 nm which is beyond our detection system. To map the $4p^5 5p \rightarrow 4p^5 5$ s transitions in the emission spectrum of krypton, different sets of data were recorded at variable discharge currents, varied from 1 to 7 mA in 1 mA steps. This current range was selected to prevent the detector saturation. In order to elucidate the levels designation of $4p^5 5p \rightarrow 4p^5 5$ s configuration, in figure 1, we have drawn the energy level diagram. The level designation of ten upper and four ground levels of neutral krypton is depicted in the $J_c K$ coupling scheme. However, on the extreme right of figure 1, we have listed the number of allowed transitions from each upper level to the lower levels.

In figure 2, we present the spectrum covering the spectral region from 750 to 840 nm, showing the prominent lines of Krypton. Interestingly, most of the intense lines of krypton exist in this wavelength region. These spectral lines are well
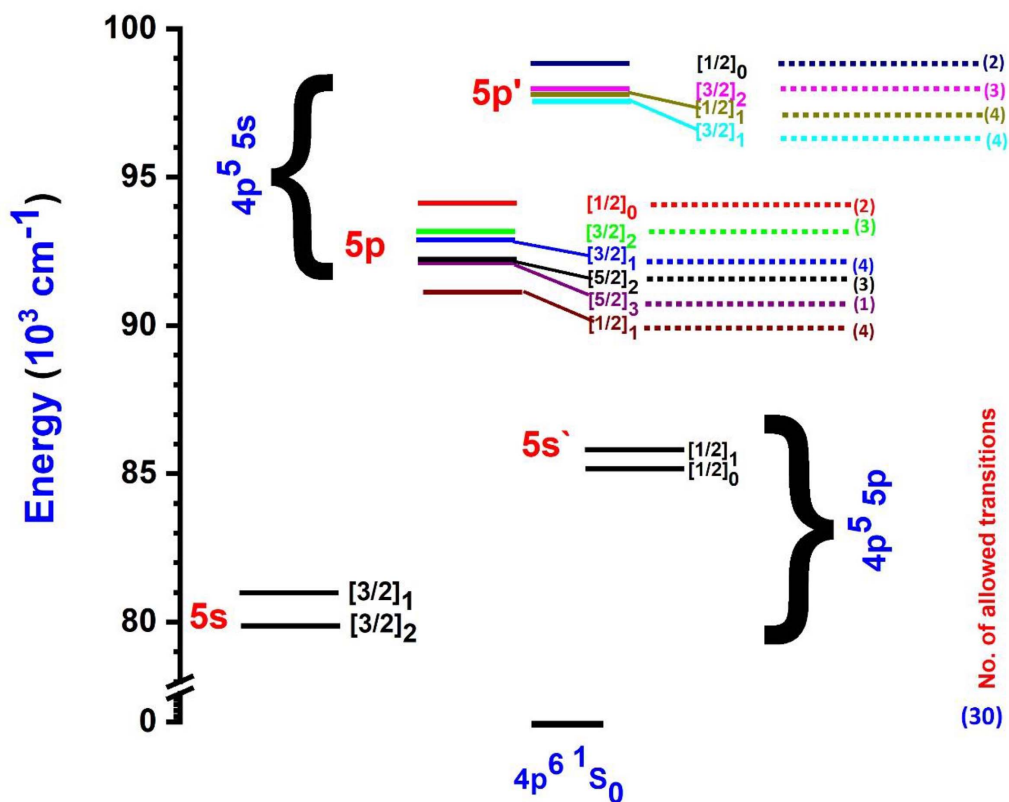
Figure 1

Energy (10^3 cm^{-1})

100

95

90

85

80

0

$4p^5\,5s$

5p'

5p

[1/2]$_0$ .... (2)
[3/2]$_2$ .... (3)
[1/2]$_1$ .... (4)
[3/2]$_1$ .... (4)

[1/2]$_0$ .... (2)
[3/2]$_2$ .... (3)
[3/2]$_1$ .... (4)
[5/2]$_2$ .... (3)
[5/2]$_3$ .... (1)
[1/2]$_1$ .... (4)

5s`

[1/2]$_1$
[1/2]$_0$

$4p^5\,5p$

No. of allowed transitions

(30)

5s

[3/2]$_1$
[3/2]$_2$

$4p^6\,{}^1S_0$

Figure 1. The diagram of the upper ($4p^5 5p$) and lower ($4p^5 5\,s$) configurations based levels of neutral Krypton.

Figure 2

Intensity (a.u)

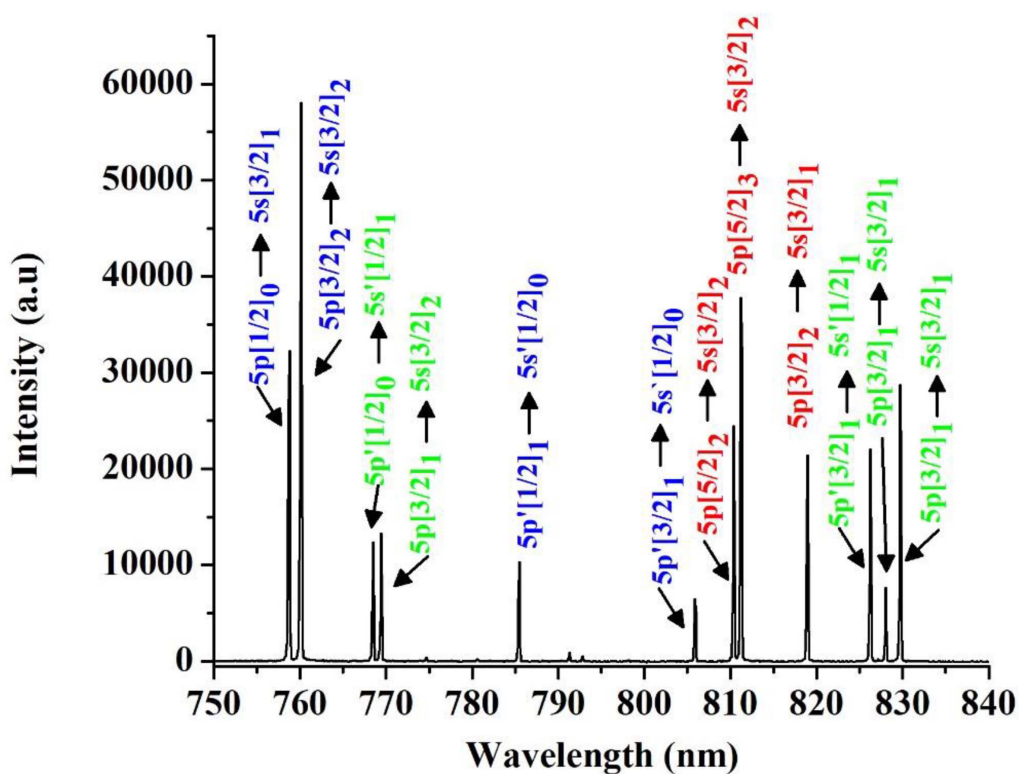60000

50000

40000

30000

20000

10000

0

750   760   770   780   790   800   810   820   830   840

Wavelength (nm)

5p[1/2]$_0$ → 5s[3/2]$_1$
5p[3/2]$_2$ → 5s[3/2]$_2$
5p'[1/2]$_0$ → 5s'[1/2]$_1$
5p[3/2]$_1$ → 5s[3/2]$_2$
5p'[1/2]$_1$ → 5s'[1/2]$_0$
5p'[3/2]$_1$ → 5s'[1/2]$_0$
5p[5/2]$_2$ → 5s[3/2]$_2$
5p[5/2]$_3$ → 5s[3/2]$_2$
5p[3/2]$_2$ → 5s[3/2]$_1$
5p'[3/2]$_1$ → 5s'[1/2]$_1$
5p[3/2]$_1$ → 5s[3/2]$_1$
5p[3/2]$_1$ → 5s[3/2]$_1$

Figure 2. Emission spectrum of krypton covering the wavelength range between 750 and 840 nm.

Krypton Transitions J_cK Designation	Paschen Notations	λ (Vac.) (nm)	This Work Experimental BF	Dzierzega *et al* [17] Experimental BF
5p'[1/2]$_0$→5 s'[1/2]$_1$	2p$_1$→1s$_2$	768.736	–	0.999 [a]
→5 s[3/2]$_1$	→1s$_4$	557.465	–	0.001 [a]
5p'[3/2]$_2$→5 s'[1/2]$_1$	2p$_2$→1s$_2$	826.551	0.975 ± 0.078	0.977 ± 0.0 05 [a]
→5 s[3/2]$_1$	→1s$_4$	587.254	0.021 ± 0.002	0.020 ± 0.004 [a]
→5 s[3/2]$_2$	→1s$_5$	556.377	0.004 ± 0.0003	0.003 ± 0.004 [a]
	2p$_3$→1s$_2$	828.333	0.390 ± 0.031	0.398 ± 0.014 [a]
5p'[1/2]$_1$→5 s'[1/2]$_1$				
→5 s'[1/2]$_0$	→1s$_3$	785.698	0.600 ± 0.048	0.573 ± 0.008 [a]
→5 s[3/2]$_1$	→1s$_4$	588.153	0.003 ± 0.0002	0.002 ± 0.0002 [a]
→5 s[3/2]$_2$	→1s$_5$	557.184	0.0070 ± 0.0006	0.028 ± 0.0016 [a]
5p'[3/2]$_1$→5 s'[1/2]$_1$	2p$_4$−1s$_2$	851.121	0.534 ± 0.0427	0.533 ± 0.015 [a]
→5 s'[1/2]$_0$	→1s$_3$	806.172	0.459 ± 0.037	0.465 ± 0.014 [a]
→5 s[3/2]$_1$	→1s$_4$	599.551	0.004 ± 0.0003	0.0015 ± 0.0002 [a]
→5 s[3/2]$_2$	→1s$_5$	567.403	0.0027 ± 0.0002	0.00044 ± 0.0001 [a]
5p[1/2]$_0$→5 s'[1/2]$_1$	2p$_5$→1s$_2$	1212.686	–	0.003560 ± 0003 [b]
→5 s[3/2]$_1$	→1s$_4$	758.950	–	0.9965 ± 0.0033 [b]
5p[3/2]$_2$→5 s[1/2]$_1$	2p$_6$→1s$_2$	1374.261	–	0.008360 ± 0003 [b]
→5 s[3/2]$_1$	→1s$_4$	819.231	0.262 ± 0.021	0.248 ± 0.009 [a]
→5 s[3/2]$_2$	→1s$_5$	760.364	0.738 ± 0.059	0.743 ± 0.007 [a]
5p[3/2]$_1$→5 s[1/2]$_1$	2p$_7$→1s$_2$	1404.950	–	0.002360 ± 0001 [b]
→5 s'[1/2]$_0$	→1s$_3$	1286.541	–	0.003160 ± 0002 [b]
→5 s[3/2]$_1$	→1s$_4$	830.039	0.80 ± 0.064	0.868 ± 0.005 [a]
→5 s[3/2]$_2$	→1s$_5$	769.666	0.202 ± 0.016	0.127 ± 0.004 [a]
5p[5/2]$_2$→5 s'[1/2]$_1$	2p$_8$→1s$_2$	1547.826	–	0.002660 ± 0001 [b]
→5 s[3/2]$_1$	→1s$_4$	877.916	0.692 ± 0.055	0.709 ± 0.01 [a]
→5 s[3/2]$_2$	→1s$_5$	810.659	0.308 ± 0.025	0.288 ± 0.015 [a]
5p[5/2]$_3$→5 s[3/2]$_2$	2p$_9$→1s$_5$	811.513	–	1
5p[1/2]$_1$→5 s'[1/2]$_1$	2p$_{10}$→1s$_2$	1879.059	–	0.002860 ± 0001 [b]
→5 s'[1/2]$_0$	→1s$_3$	1673.108	–	0.004860 ± 0002 [b]
→5 s[3/2]$_1$	→1s$_4$	975.444	0.129 ± 0.010	0.120 ± 0.004 [b]
→5 s[3/2]$_2$	→1s$_5$	893.114	0.871 ± 0.070	0.873 ± 0.004 [a]

[a]Wall-stabilized arc measurement
[b]Hollow-cathode lamp measurement.

resolved; therefore, it was convenient to extract information about their BF, transition probabilities, and relative line strengths.

3.2. Determination of branching fractions

The BF of nineteen spectral lines of neutral krypton attached to the $4p^55p$ to $4p^55$ s configurations-based levels have been determined. Accurate measurements of the BF are very crucial for the precise determination of the transition rates. BF can be determined from the measured relative intensities of the emission lines originating from a common upper level and terminating on different lower levels and dividing it by the sum of the intensities of all the involved spectral lines. To calculate the BF, the strength of spectral lines was determined by measuring the area under the curves. The BF of the transitions originating from a common upper and terminating on lower levels are calculated using the relation [21]:

$$BF_i = \frac{I_i}{\sum\limits_k I_k}. \tag{1}$$

Here, numerator represents the intensity of the individual line for which the branching fraction is to be determined and denominator is the sum of the intensities of all the lines from a common upper level and terminating on lower levels.

The experimental BF obtained for the krypton spectral lines are listed in table 1. In columns one and two, we enlist the transitions in the j_cK coupling scheme and in Paschen notations, the third column contains transition wavelengths, the fourth and fifth columns consist of the present data on BF and its comparison with the experimentally measured values [17], respectively. Our experimentally determined BF are in good agreement with that listed values [17].

3.3. Determination of absolute transition probabilities and their comparison with intermediate coupling calculations

The transition probability of any spectral lines is related to the lifetime of the upper level. Thus, by combining the lifetime of an upper level with the branching fractions of all the spectral lines connected with the upper level, one can determine

Table 2. Absolute transition probabilities of Kr I for $4p^5 5p \rightarrow 4p^5 5s$.

Krypton Transitions J_cK Designation	Paschen Notations	λ (Vac.) (nm)	Life Times τ (ns)	This Work $A_{ki} \times 10^6$ (s^{-1})	Milosavlevic et al [20] $A_{ki} \times 10^6$ (s^{-1})	NIST Database [18] $A_{ki} \times 10^6$ (s^{-1})	Theoretical Trans. Prob. $A_{ki} \times 10^6$ (s^{-1}) Aymar and Coulombe [10] Length	Velocity
5p'[1/2]$_0$→5 s'[1/2]$_1$	2p$_1$→1s$_2$	768.736	22.1 ± 2[a]	43.9 ± 4.1	49	40.64	49.6	32.9
→5 s[3/2]$_1$	→1s$_4$	557.465		—	—	—	0.437	0.251
5p'[3/2]$_2$→5 s'[1/2]$_1$	2p$_2$→1s$_2$	826.551	26.9 ± 0.3[b]	36.2 ± 3.9	35	34.16	41.1	32.2
→5 s[3/2]$_1$	→1s$_4$	587.254		0.79 ± 0.09	1.8	0.71	2.39	0.933
→5 s[3/2]$_2$	→1s$_5$	556.377		0.16 ± 0.02	0.3	0.11	0.595	0.201
5p'[1/2]$_1$→5 s'[1/2]$_2$	2p$_3$→1s$_2$	828.333	26.8 ± 1.7[b]	14.6 ± 2.2	21.1	14.18	18.8	14.7
→5 s'[1/2]$_0$	→1s$_3$	785.698		22.4 ± 3.4	25.8	20.41	28.4	18
→5 s[3/2]$_1$	→1s$_4$	588.153		0.112 ± 0.017	—	0.055	0.198	0.0848
→5 s[3/2]$_2$	→1s$_5$	557.184		0.260 ± 0.039	—	0.98	3.91	1.32
5p'[3/2]$_1$→5 s'[1/2]$_1$	2p$_4$→1s$_2$	851.121	27.2 ± 1.6[b]	19.6 ± 2.8	17.7	18.11	20.6	17.1
→5 s'[1/2]$_0$	→1s$_3$	806.172		16.9 ± 2.7	—	15.83	21.2	15.8
→5 s[3/2]$_1$	→1s$_4$	599.551		0.15 ± 0.02	—	0.05	0.0841	0.0397
→5 s[3/2]$_2$	→1s$_5$	567.403		0.1 ± 0.02	—	0.015	0.455E-02	0.158E-02
5p[1/2]$_0$→5 s'[1/2]$_1$	2p$_5$→1s$_2$	1212.686	22.8 ± 2[a]	—	—	0.150	0.143E-02	0.0407E-02
→5 s[3/2]$_1$	→1s$_4$	758.950		43.9 ± 6.6	—	43.10	52.4	33.8
5p[3/2]$_2$→5 s'[1/2]$_1$	2p$_6$→1s$_2$	1374.261	27.35 ± 0.06[c]	—	—	0.31	0.164	0.356
→5 s[3/2]$_1$	→1s$_4$	819.231		9.6 ± 0.7	11.5	8.94	11.6	8.88
→5 s[3/2]$_2$	→1s$_5$	760.364		27.0 ± 2.2	31	27.32	38.6	25.5
5p[3/2]$_1$→5 s'[1/2]$_1$	2p$_7$→1s$_2$	1404.950	29.51 ± 0.06[c]	—	—	0.106	0.0633	0.141
→5 s'[1/2]$_0$	→1s$_3$	1286.541		—	—	0.076	0.0345	0.0664
→5 s[3/2]$_1$	→1s$_4$	830.039		26.8 ± 2.2	34.2	29.31	36	28.3
→5 s[3/2]$_2$	→1s$_5$	769.666		7.1 ± 0.6	6.2	4.27	6.82	4.42
5p[5/2]$_2$→5 s'[1/2]$_1$	2p$_8$→1s$_2$	1547.826	32.10 ± 0.09[c]	—	—	0.081	0.0477	0.131
→5 s[3/2]$_1$	→1s$_4$	877.916		18.8 ± 1.7	—	22.17	25.1	22.2
→5 s[3/2]$_2$	→1s$_5$	810.659		12.4 ± 0.8	13	8.96	12.6	9.50
5p[5/2]$_3$→5 s[3/2]$_2$	2p$_9$→1s$_5$	811.513	27.73 ± 0.07[c]	36.1 ± 2.9	38.6	36.10	44.6	33.7
5p[1/2]$_1$→5 s'[1/2]$_1$	2p$_{10}$→1s$_2$	1879.059	40.9 ± 1.7[b]	—	—	0.074	0.0344	0.143
→5 s'[1/2]$_0$	→1s$_3$	1673.108		—	—	0.126	0.0617	0.201
→5 s[3/2]$_1$	→1s$_4$	975.444		3.16 ± 0.25	—	3.13	3.43	3.75
→5 s[3/2]$_2$	→1s$_5$	893.114		21.3 ± 1.7	—	22.89	28.4	26.1

[a] Fonseca and Campos [11]

[b] Chang et al [13]
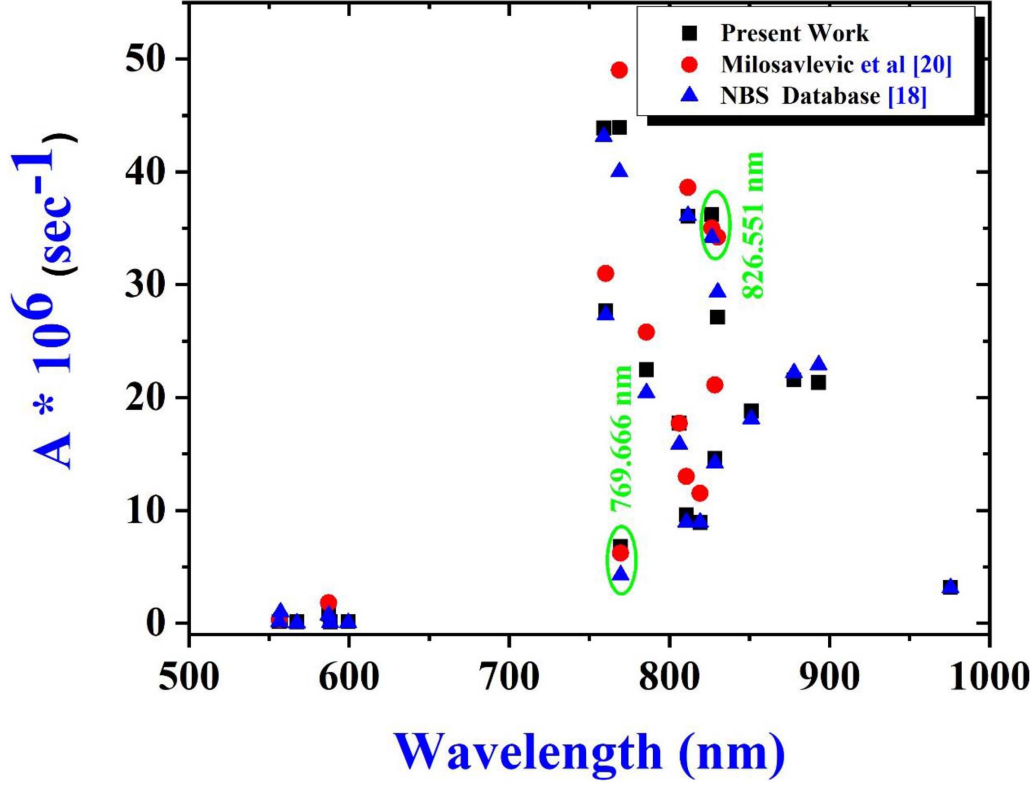
[c] Schmoraner and Völz [16]

Figure 3. A comparison of the present measurements (solid black squares), solid red circles [20] and solid blue triangles NIST Database [18] versus wavelength.

the transition probabilities of all the lines. In order to measure the absolute transition probability A_{ki} from an upper level i to lower level k, it is important that the lifetime of the upper level τ_i is precisely known and BF are available which are related as [22]:

$$A_{ik} = \frac{BF_i}{\tau_i} \qquad (2)$$

where, BF_i is the experimentally measured branching fraction and τ_i is the experimentally reported life time of the upper level. The lifetimes of the upper levels attached to the $4p^5 5p$ configuration have been reported in the literature [11, 13, 16] have been used to deduce the transition probabilities for each multiplet. The lifetimes of the 5p'[1/2]$_0$ and 5p'[3/2]$_1$, levels are missing in [13]. therefore, we have taken these values from [12]. The upper levels lifetimes listed in column four contain some uncertainties. The maximum uncertainty is ~9% for the 5p'[1/2]$_0$ and 5p'[1/2]$_1$ level whereas, the minimum uncertainty is ~1% for the 5p'[3/2]$_1$ level. The uncertainties are attributed to the errors associated with the measured lifetimes of the upper levels (1%–10%) and to that in the measured line intestines (5%–8%). The overall uncertainty in the measured data is ⩽15%. The reported lifetime's uncertainties in the individual upper level along with the uncertainties in the BF have been added in the deduced transition probabilities. In table 2, the first, second and third column enlists the optically allowed transitions in J_ck coupling, Paschen notations and transition wavelengths. The lifetimes of upper levels

are given in the fourth column whereas, the transition probabilities measured in this work are listed in the fifth column. In the last three columns, we have compared our data with the experimentally measured [18, 20] and theoretically calculated [10], based on the intermediate coupling theory, respectively. A graphical comparison of transition probabilities as a function of wavelength measured in this work, experimentally reported values [20] and that in the NIST Database [18] is depicted in figure 3. The transition probabilities data for the 5p'[1/2]$_0$→5 s[3/2]$_1$ transition line is missing in our measurements as well as in the NIST database [18]. Recently, the transition probabilities were reported for a few lines of Kr I [20] but the data for the nine Kr I lines (588.153, 557.184, 851.121, 599.551, 567.403, 758.950, 877.916, 975.444 and 893.114 nm), were not reported. These lines along with their wavelengths are shown in figure 3. There is a very small difference between our measurements and that reported in [20] (refer figure 3 with green circles). However, much improved values for the other twenty lines have been extracted in the present work. The percentage differences of ten lines between the NIST database [18] and the present measurements remain less than 10%. However, percentage difference for the weak intensity lines (556.377, 588.153, 557.184, 599.551 and 567.403 nm) are higher than that reported in NIST Database [18]. These differences may be attributed to the errors in the measurements of the line intensities from the observed spectrum. Furthermore, a couple of strong lines at 769.666 and 810.437 nm also show much higher difference with NIST

Table 3. Relative line strengths of Kr I for $4p^55p \rightarrow 4p^55$ s.

Krypton Transitions J_cK Designation	Paschen Notations	λ (Vac.) (nm)	Line Strength This Work S_{ij} (a.u)	NIST Database [18] S_{ij} (a.u)	Theoretical Line Strength S_{ij} (a.u) Aymar and Coulombe [10]	
					Length	*Velocity*
5p'[1/2]$_0\rightarrow$5 s'[1/2]$_1$	2p$_1\rightarrow$1s$_2$	768.736	9.85 ± 1.48	9.11	11.1	7.39
$\rightarrow$5 s[3/2]$_1$	$\rightarrow$1s$_4$	557.465	—	—	0.100E01	0.338
5p'[3/2]$_2\rightarrow$5 s'[1/2]$_1$	2p$_2\rightarrow$1s$_2$	826.551	50.48 ± 4.54	47.60	57.3	44.8
$\rightarrow$5 s[3/2]$_1$	$\rightarrow$1s$_4$	587.254	0.40 ± 0.36	0.90	1.19	0.466
$\rightarrow$5 s[3/2]$_2$	$\rightarrow$1s$_5$	556.377	0.067 ± 0.050	0.047	0.253	0.0853
5p'[1/2]$_1\rightarrow$5 s'[1/2]$_1$	2p$_3\rightarrow$1s$_2$	828.333	12.25 ± 1.91	11.93	15.8	12.4
$\rightarrow$5 s'[1/2]$_0$	$\rightarrow$1s$_3$	785.698	16.08 ± 2.31	14.66	18.3	12.9
$\rightarrow$5 s[3/2]$_1$	$\rightarrow$1s$_4$	588.153	0.034 ± 0.008	1.66E-02	0.0598	0.0255
$\rightarrow$5 s[3/2]$_2$	$\rightarrow$1s$_5$	557.184	0.067 ± 0.31	0.251	1	0.338
5p'[3/2]$_1\rightarrow$5 s'[1/2]$_1$	2p$_4\rightarrow$1s$_2$	851.121	17.92 ± 1.89	16.53	18.8	15.6
$\rightarrow$5 s'[1/2]$_0$	$\rightarrow$1s$_3$	806.172	13.09 ± 1.51	12.28	16.5	12.3
$\rightarrow$5 s[3/2]$_1$	$\rightarrow$1s$_4$	599.551	0.047 ± 0.006	0.0160	0.0160	0.0127
$\rightarrow$5 s[3/2]$_2$	$\rightarrow$1s$_5$	567.403	0.027 ± 0.003	4.1E-03	0.123E-02	0.427E-03
5p[1/2]$_0\rightarrow$5 s'[1/2]$_1$	2p$_5\rightarrow$1s$_2$	1212.686	—	1.10E-03	0.126E-02	0.358E-03
$\rightarrow$5 s[3/2]$_1$	$\rightarrow$1s$_4$	758.950	9.46 ± 0.95	9.30	11.3	7.29
5p[3/2]$_2\rightarrow$5 s[1/2]$_1$	2p$_6\rightarrow$1s$_2$	1374.261	—	1.99	0.105E01	0.228E01
$\rightarrow$5 s[3/2]$_1$	$\rightarrow$1s$_4$	819.231	13 ± 1.94	12.13	15.7	12.1
$\rightarrow$5 s[3/2]$_2$	$\rightarrow$1s$_5$	760.364	29.27 ± 2.81	29.64	41.9	27.6
5p[3/2]$_1\rightarrow$5 s[1/2]$_1$	2p$_7\rightarrow$1s$_2$	1404.950	—	0.435	0.260	0.579
$\rightarrow$5 s'[1/2]$_0$	$\rightarrow$1s$_3$	1286.541	—	0.240	0.109	0.209
$\rightarrow$5 s[3/2]$_1$	$\rightarrow$1s$_4$	830.039	22.72 ± 2.53	24.82	30.5	24
$\rightarrow$5 s[3/2]$_2$	$\rightarrow$1s$_5$	769.666	4.76 ± 0.51	2.88	4.40	2.98
5p[5/2]$_2\rightarrow$5 s'[1/2]$_1$	2p$_8\rightarrow$1s$_2$	1547.826	—	0.74	0.436	0.120E01
$\rightarrow$5 s[3/2]$_1$	$\rightarrow$1s$_4$	877.916	31.38 ± 3.95	37.02	42	37.1
$\rightarrow$5 s[3/2]$_2$	$\rightarrow$1s$_5$	810.659	16.25 ± 1.39	11.78	16.6	12.5
5p[5/2]$_3\rightarrow$5 s[3/2]$_2$	2p$_9\rightarrow$1s$_5$	811.513	66.62 ± 2	66.7	82.4	62.2
5p[1/2]$_1\rightarrow$5 s'[1/2]$_1$	2p$_{10}\rightarrow$1s$_2$	1879.059	—	0.727	0.338	0.140E01
$\rightarrow$5 s'[1/2]$_0$	$\rightarrow$1s$_3$	1673.108	—	0.874	0.428	0.139E01
$\rightarrow$5 s[3/2]$_1$	$\rightarrow$1s$_4$	975.444	4.33 ± 0.48	4.30	4.71	5.16
$\rightarrow$5 s[3/2]$_2$	$\rightarrow$1s$_5$	893.114	22.46 ± 2.47	24.14	30	27.5

Database [18]. However, the overall comparison of the transition probabilities between the presently measured values and that of listed in the literature is quite good. The theoretical transition probabilities, oscillator strengths and relative line strengths were reported in both length and velocity operator formulation [10]. Several authors have calculated the transition probabilities of the rare gases in the intermediate coupling scheme [8, 10]. In table 3, our experimentally measured transition probabilities agree well with that of theoretically calculated results which further confirms that the intermediate coupling scheme is more appropriate for the level designation of the $4p^55$ s$\rightarrow 4p^55p$ transitions array in Kr I.

3.4. Determination of experimental line strengths and testing of J-File sum rule

In this section, we present the relative line strengths for the $4p^55p \rightarrow 4p^55$ s transitions array in krypton. The purpose to determine the relative line strengths is to test the validation of the J-file sum rule. The relative line strengths of the optically allowed transitions of krypton are determined by using the general relation [23]

$$S_{ki} = 4.935 \times 10^{-19} \lambda_{ki}^3 g_k A_{ki} \qquad (3)$$

where, λ_{ki} is the wavelength in vacuum (in angstroms), g_k is the statistical weight of the respective upper level of the transition and A_{ki} is the transition probability in sec^{-1}.

The J-file sum rule provide us an analysis that how much our experimental measurements are closed to that of theoretical calculations. The numerical values of the relative line strengths are listed in table 3 that are compared with the NIST Database [18] and the theoretical line strength in both length and velocity formulation [10] showing good agreement. The J-file sum rule provides theoretical line strengths that can be used to test the experimentally obtained line strengths [24]. To the best of our knowledge, for the first time we are comparing the measured and calculated line strengths for the complete set of spectral lines belonging to the $4p^55p \rightarrow 4p^55$ s transition array. Table 4 shows the comparison of the data for the ten upper levels originating from the $4p^55p$ configuration

Table 4. Comparison of experimental line strength with normalized line strength and testing of *J*-file sum rule.

Upper Levels Paschen Notation	$J_C K$ Levels	$2J+1$	Experimental Line Strength	*J*-file sum	% Difference
2p$_1$	**5p´[1/2]$_0$**	1	9.85	9.46	4.12
2p$_2$	**5p´[3/2]$_2$**	5	50.947	47.30	7.71
2p$_3$	**5p´[1/2]$_1$**	3	28.431	28.38	0.18
2p$_4$	**5p´[3/2]$_1$**	3	31.084	28.38	9.53
2p$_5$	**5p[1/2]$_0$**	1	9.46	9.46	0
2p$_6$	**5p[3/2]$_2$**	5	42.27	47.40	−10.8
2p$_7$	**5p[3/2]$_1$**	3	27.48	28.38	−3.17
2p$_8$	**5p[5/2]$_2$**	5	47.63	47.30	0.7
2p$_9$	**5p[5/2]$_3$**	7	66.62	66.22	0.6
2p$_{10}$	**5p [1/2]$_1$**	3	26.8	28.38	−5.57
	Σ	**36**	**340.57**	**340.57**	
Lower Levels Paschen Notation	$J_C K$ Levels	$2J+1$	Experimental Line Strength	*J*-file sum	% Difference
1s$_2$	**5 s´[1/2]$_1$**	3	90.5	85.14	6.3
1s$_3$	**5 s´[1/2]$_0$**	1	29.17	28.38	2.78
1s$_4$	**5 s[3/2]$_1$**	3	81.37	85.14	−4.43
1s$_5$	**5 s[3/2]$_2$**	5	139.53	141.91	−1.68
	Σ	**12**	**340.57**	**340.57**	

and four lower levels associated with the $4p^5 5$ s configuration separately. There are some spectral lines that lie beyond our detection region but the line strength data of these transitions are very low and also do not contribute much in the errors. In the first and second column the respective levels in the Paschen notation and j_cK coupling scheme are given, respectively. The statistical weight ($2J+1$) of the levels is listed in column three. In column four, relative line strength is the summation over the line strengths of the transitions measured (present work). In the fifth column, the corresponding sum of the statistical weights for all the relevant upper and lower energy levels, normalized to the total sum (340.57) of the experimental line strengths is listed. In the last column, the discrepancies between the experimental line strengths and *J*-file sum rule are presented. The sum of line strengths for the upper as well as lower levels have been evaluated in this work (experimental line strength = 340.57) and compared with the corresponding sums of line strengths (experimental line strength = 340.57) determined from the *J*-file sum rule. For the upper levels, the maximum difference is observed ~ −10.8% for 5p[3/2]$_2$, while the minimum difference is found to be ~0.6% for 5p[5/2]$_3$. In the case of the lower levels, the highest difference is ~6.3% for 5 s' [1/2]$_1$ and lowest difference is about ~ −1.68% for 5 s[3/2]$_2$. All these differences are attributed to the measured relative line strengths from the transition probabilities, thus the errors which are present in the transition probabilities data also contribute in the relative line strengths. In addition, the relative line strength data for few transitions, which are beyond the range of our spectrometer, are missing which consequences some discrepancies between the experimental data and normalized *J*-file sum rule. Such an analysis has been reported for the case of neon [25, 26], where we determined the experimental transition probabilities and relative line strengths for all the optically allowed transitions belonging to the $2p^5 3p \rightarrow 2p^5 3$ s transition array. In addition, a J-file sum rule test was also performed for the 3 s→3p transition array in the singly ionized nitrogen and good comparison was found between the measured and calculated data [27]. The line strengths calculated from the *J*-file sum rule are very close to that our experimentally determined values and may be used for the plasma diagnostics. More recently, Javed *et al* [28], reported the line strengths for the $4p5$ s $^3P_{0,1,2} \rightarrow 4p^2{}^3P_{0,1,2}$ transitions and compared the data with that calculated in the LS coupling scheme revealing that the intermediate coupling scheme is more appropriate for the level designation in germanium.

4. Conclusion

In this experiment, the emission spectrum of krypton was recorded by using a krypton hollow cathode lamp covering the wavelength range from 500 nm to 1000 nm. The BF of the krypton have been measured by the intensity ratios of the integrated spectral lines. The set of experimental transition probabilities of twenty two spectral lines of krypton attached to the $4p^5 5p \rightarrow 4p^5 5$ s transition array were computed by combining the branching factions with the lifetimes of the upper levels. The measured branching fractions, transition probabilities, and relative line strengths were in close agreement with the published experimental as well as theoretical data. The experimental line strengths were used to test the validity of *J*-file sum rule by comparing the measured experimental line strengths with the normalized theoretical statistical weight. The resulting differences between the theoretical and the experimental measurements were discussed for all the measured spectroscopic parameters.

Acknowledgments

References

[1] Demtroder W 2003 *Laser Spectroscopy: Basic Concepts and Instrumentation* 3rd edn (New York: Springer)

[2] Cowan R W 1981 *The Theory of Atomic Structure and Spectra* (Berkeley, CA: University of California Press)

[3] Axner O, Gustafsson J, Omenetto N and Winefordner J D 2004 Line strengths, *A*-factors and absorption cross-sections for fine structure lines in multiplets and hyperfine structure components in lines in atomic spectrometry—a user's guide *Spectrochim. Acta* B **59** 1–39

[4] Thorne A P and Chamberlain J E 1963 Transition probabilities in the spectra of neutral Neon, Argon and krypton *Proc. Phys. Soc.* **82** 133–41

[5] Murphy P W 1968 Transition probabilities in the spectra of Ne I, Ar I and Kr I *J. Opt. Soc. Am.* **58** 1200–8

[6] Aymar M, Feneuille S and Klapisch M 1970 Theoretical transition probabilities and lifetimes in noble gas spectra *Nucl. Instrum. Methods* **90** 137–43

[7] Miller M H and Roig R A 1972 Relative transition probabilities of Krypton *J. Opt. Soc. Am.* **62** 1027–9

[8] Lilly R A 1976 Transition probabilities in the spectra of Ne I, Ar I and Kr I *J. Opt. Soc. Am.* **66** 245–9

[9] Ernst W E and Schulz-gulde E 1978 Transition probabilities for Kr I lines from wall-stabilized arc measurements *Physica* B+C **93** 136–44

[10] Aymar M and Coulombe M 1978 Theoretical transition probabilities and lifetimes in Kr I and Xe I spectra *At. Data Nucl. Data Tables* **21** 537–66

[11] Fonseca V and Campos J 1978 Lifetimes of some levels belonging to the $4p^5 5p$ and $4p^5 6p$ configurations of Kr I *Phys. Rev.* A **17** 1080

[12] Fonseca V and Campos J 1979 Absolute transition probabilities of some Kr I lines *Physica* B+C **97** 312–14

[13] Chang R S F, Horiguchi H and Setser D W 1980 Radiative lifetimes and two-body collisional deactivation rate constants in argon for Kr($4p^5 5p$) and Kr ($4p^5 5p'$) states *J. Chem. Phys.* **73** 778–90

[14] Peraza C, Martin P and Campos J 1991 Transition probabilities of infrared lines 6p-6s and 5p-4d of Kr I *J. Quant. Spectrosc. Radiat. Transfer* **45** 63–68

[15] Cannon B D, Glab W L and Ogorzalek L R 1993 Photoionization cross section of the $4p^5 5d[7/2]J=4$ state and radiative lifetimes of three states of Kr I *Phys. Rev.* A **47** 147–52

[16] Schmoranzer H and Volz U 1993 Atomic lifetime measurements by beam-gas-dye laser spectroscopy *Phys. Scr.* **T47** 42–48

[17] Dzierzega K, Volz U, Nave G and Griesmann U 2000 Accurate transition rates for the 5p−5s transitions in Kr I *Phys. Rev.* A **62** 22505

[18] NIST *Atomic Spectra Database* (available at: http://physics.nist.gov)

[19] Rodrguez F, Aparicio J A, Castro A D, Val J A D, Gonzalez V R and Mar S 2001 Measurement of several transition probabilities in singly-ionized krypton *Astron. Astrophys.* **372** 338–45

[20] Milosavljevic V, Simic Z, Daniels S and Dimitrijevic M S 2012 Stark shifts and transition probabilities within the Kr I spectrum *Mon. Not. R: Astron. Soc.* **422** 610–18

[21] Curtis L 2003 *Atomic Structure and Lifetimes* (Cambridge: Cambridge University Press)

[22] Xu H L, Sun Z W, Dai Z E, Jiang Z K, Palmeri P, Quinet P and Biemont E 2006 Radiative lifetimes, branching fractions and oscillator strengths in Pd I and the solar palladium abundance *Astron. Astrophys.* **452** 357–62

[23] Wiese W L, Fuhr J R and Deters T M 1996 Atomic transition probabilities of carbon, nitrogen, and oxygen: a critical data compilation *J. Phys. Chem. Ref. Data, Monograph* **7** 1–52

[24] Baclawski A 2008 Experimental transition probabilities and J-file sum rule test for the transition array 3p–3d in neutral neon *J. Phys. B: At. Mol. Opt. Phys.* **41** 225701

[25] Asghar H, Ali R and Baig M A 2013 Determination of transition probabilities for the 3p→3s transition array in neon using laser induced breakdown spectroscopy *Phys. Plasmas* **20** 123302

[26] Piracha N K, Duncan-Chamberlin K V, Kaminsky J, Delanis D, Asghar H, Ali R and Baig M A 2015 Transition probabilities, oscillator strengths, and test of *J*-file sum rule for the $2p^5 3p$-$2p^5 3s$ transition array in the neon emission spectra *Can. J. Phys.* **93** 80–4

[27] Musielok J 2005 J-File Sum Rule Tests for the 3s-3p transition array in singly ionized nitrogen | comparison of measured and calculated data *Acta Phys. Pol.* A **108** 449–56

[28] Iqbal J, Ahmed R and Baig M A 2017 Time integrated optical emission studies of the laser produced germanium plasma *Laser Phys.* **27** 046101